Canadian Mineralogist
Vol. 29, pp. 533-541 (1991)

YTTRIAN MILARITE

PETR ČERNÝ AND FRANK C. HAWTHORNE
Department of Geological Sciences, University of Manitoba, Winnipeg, Manitoba R3T 2N2

JOHN L. JAMBOR
CANMET, 555 Booth Street, Ottawa, Ontario K1A 0G1

JOEL D. GRICE
Mineral Sciences Section, Canadian Museum of Nature, Ottawa, Ontario K1P 6P4

ABSTRACT

Milarite from the Jaguaraçú pegmatite, Minas Gerais, Brazil, and from the Strange Lake peralkaline complex, Labrador–Québec border, contains up to 7.90 wt.% Y_2O_3 and 5.10 wt.% ΣREE_2O_3. The Strange Lake milarite shows moderate concentric or sector zoning. The Jaguaraçú milarite shows enrichment in (Y,*REE*) in the outermost zones, in networks of fracture-filling and replacement veinlets of a (Y,*REE*)-rich phase in the primary (Y,*REE*)-poor interior, and, to a degree, in (Y,*REE*)-poor pinacoidal caps. The principal substitution is that of $^{A}Y,REE^{3+} + {}^{T(2)}Be^{2+} \rightleftharpoons {}^{A}Ca^{2+} + {}^{T(2)}Al^{3+}$, leading from the ideal composition $KCa_2(Be_2Al)Si_{12}O_{30}$ to $K(CaY)(Be_3)Si_{12}O_{30}$. However, the *A* position also shows minor vacancies (<9%) that increase with the (Y,*REE*) content. The above substitution strongly modifies intensities of X-ray diffraction maxima, and reduces the unit-cell dimensions. Additional occurrences of yttrian milarite can be expected in (Y,*REE*)-rich miarolitic peralkaline intrusions and related hydrothermal environments. An extension of the substitution from $K(CaY)(Be_3)Si_{12}O_{30}$ to $(Y_2)(Be_3)Si_{12}O_{30}$ is a possibility.

Keywords: milarite, yttrium, rare-earth elements, Labrador, Brazil.

SOMMAIRE

La milarite de la pegmatite de Jaguaraçú, à Minas Gerais au Brésil, et du complexe hyperalcalin de Strange Lake, sur la frontière Québec–Labrador, contient jusqu'à 7.90% de Y_2O_3 (en poids) et 5.10% en oxydes de terres rares. La milarite de Strange Lake montre une zonation, soit concentrique, soit en secteurs. Celle de Jaguaraçú montre un enrichissement en Y et les terres rares vers les zones externes, et dans un réseau de micro-fissures et de veinules de remplacement d'une phase riche en Y et terres rares dans les secteurs internes et le pinacoïde apical, à faibles teneurs en Y et terres rares. La substitution principale serait $^{A}(Y,\text{ terres rares})^{3+} + {}^{T(2)}Be^{2+} \rightleftharpoons {}^{A}Ca^{2+} + {}^{T(2)}Al^{3+}$, qui définit un intervalle de compositions entre $KCa_2(Be_2Al)Si_{12}O_{30}$ et $K(CaY)(Be_3)Si_{12}O_{30}$. Toutefois, la position *A* peut contenir une légère proportion de lacunes (<9%), qui augmente avec la proportion d'yttrium et de terres rares. Cette substitution couplée modifie fortement les intensités des raies dans un cliché de diffraction X, et mène à une réduction des paramètres réticulaires. On peut s'attendre à d'autres exemples de milarite yttrifère dans les cavités miarolitiques de complexes intrusifs hyperalcalins riches en Y et terres rares, ainsi que dans les milieux hydrothermaux qui leurs sont associés. Une extension du schéma de substitution du pôle $K(CaY)(Be_3)Si_{12}O_{30}$ au pôle $(Y_3)(Be_3)Si_{12}O_{30}$ peut être envisagée.

(Traduit par la Rédaction)

Mots-clés: milarite, yttrium, terres rares, Labrador, Brésil.

INTRODUCTION

The double-ring silicate *milarite*, ideally $^{C(B)}(K,Na)^{A}Ca_2{}^{T(2)}(Be_2Al)^{T(1)}Si_{12}O_{30}{}^{B(D?)}H_2O$, was described as a new mineral species 130 years ago; the complex history of its study was reviewed by Černý *et al.* (1980; see their Fig. 1 for structure and site symbolism). These authors recognized a wide range of Be/Al proportions in this mineral, from about $(Be_{1.9}Al_{1.1})$ to $(Be_{2.55}Al_{0.45})$, resulting from the substitution

$$^{T(2)}Be^{2+} + {}^{C(B)}(Na,K)^{+} \rightleftharpoons {}^{T(2)}Al^{3+} + {}^{C(B)}\square.$$

These authors also reviewed the relationships among structure, chemistry, unit-cell dimensions, and optical properties in both natural and heated specimens of milarite from 16 localities. Additional data on milarite have been reported recently by Janeczek (1986), Armbruster *et al.* (1989) and Kimata & Hawthorne (1989).

Yttrium was reported in trace to minor quantities in milarite from several localities (Sosedko 1960, Černý 1960, 1967, 1968, Sosedko & Telesheva 1962, Stanèk 1964, Chistyakova *et al.* 1964, Iovcheva *et al.* 1966, Novikova 1972). However, significant

yttrium content, estimated by emission spectrographic analysis, was known only for the milarite from Grorud, Norway (Oftedal & Saebø 1965).

In 1986, one of us (J.L.J.) obtained electron-microprobe data on milarite from the Strange Lake peralkaline complex, Québec–Labrador border, which turned out to have high levels of Y, *REE* and (calculated) Be, but low Ca and Al contents, and unit-cell dimensions distinctly different from the previously established range. Recently, we recorded analogous unit-cell dimensions, and an unusual distribution of X-ray powder-diffraction intensities, for a milarite sample from the Jaguaraçú granitic pegmatite, Brazil (supplied by Dr. R.V. Gaines). As this locality is famous for its high concentration of Y (Foord *et al.* 1986), enrichment of milarite in Y was considered a distinct possibility.

We report here the results of our study on the Jaguaraçú and Strange Lake samples of milarite, both of which have proven to be Y-rich. More detailed examination of the Strange Lake milarite has shown the presence of even higher Y contents than those revealed by the 1986 analyses.

Samples Examined

At Strange Lake, Québec–Labrador border, milarite occurs in an extensively mineralized peralkaline granite, in part pegmatitic (*e.g.*, Miller 1989, Boily *et al.* 1990). The milarite is found in three associations: (i) as anhedral grains associated with quartz, albite, and K-feldspar in a medium-grained granitic assemblage that also contains armstrongite, titanite, gittinsite, aegirine and fluorite (drill core sample SL–60D–18.3); (ii) as euhedral columnar crystals with prismatic, pyramidal and basal pinacoid faces, measuring up to 0.15 × ~0.50 mm in size, in miarolitic vugs lined with quartz and albite crystals, all locally dusted with hematite (drill-core sample SL–258–71), and (iii) as clear, white, purplish to reddish euhedral columnar crystals with a well-defined dominant core and subordinate outer zones, in small vugs lined with powdery xenotime (drill-core sample SL–258–75.2).

In the Jaguaraçú pegmatite, Minas Gerais, Brazil, milarite forms pale greenish yellow or pale brown euhedral columnar crystals, up to 10 × 30 mm in size, with colorless and clear caps in pinacoidal terminations. Milarite is associated with adularia, albite, hematite, muscovite, quartz and minasgeraisite ($Y_2CaBe_2Si_2O_{10}$: Foord *et al.* 1986). Two milarite-bearing samples were examined in the present study: one with associated minasgeraisite, and the other from a specimen devoid of this Y-rich mineral.

Experimental Methods

Electron-microprobe analyses were carried out with a JEOL 733 electron microprobe, equipped with three spectrometers, utilizing an accelerating voltage of 12 kV, a beam current of 25 nA, and a beam diameter of less than 1 μm. Raw data were reduced using Tracor Northern's "Task" ZAF program. The following standards and X-ray emission lines were used: synthetic $NaNbO_3$ (Na*K*α), orthoclase (K*K*α, Al*L*α, Si*K*α), titanite (Ca*K*α), synthetic $YbFeO_3$ (Yb α), synthetic $YFeO_3$ (Y*L*α), synthetic CeO_2(Ce*L*α), synthetic $NdAlO_3$ (Nd α), synthetic $ErAlO_3$ (Er*L*α), and synthetic glass *REE4* (DyLα).

No elements were detected in quantitatively determinable amounts except those for which the X-ray emission lines are quoted here. Table 1 summarizes the localities and sample-plus-analysis numbers, and Figure 1 shows the location of different analyzed fragments of one of the Jaguaraçú specimens.

TABLE 1. LIST OF MILARITE SAMPLES

Sample #	Locality	Source	Analysis #
MI-1A, B	Jaguaraçú, Brazil; associated with minasgeraisite	R.V. Gaines	MI-1A-1, MI-1A-2 to -4; MI-1A-3-5 to -9; MI-1B-1 and 2
MI-2 to 7	Jaguaraçú, Brazil;	R.V. Gaines	MI-2-1 to -3;MI 3-1 and -2; MI-4-1 and -2; MI-5-1 and -2; MI-6-1 and -2; MI-7-1 and -2
SL-60D-18.3	Strange Lake, Labrador-Québec; thin section	J.L. Jambor	SL-60D-19.3-1 and -2
SL-258-71	Strange Lake, Labrador-Québec; crystals in vugs	J.L. Jambor	71-1 and 71-2
SL-258-75.2	Strange Lake, Labrador-Québec; crystals in vugs	J.L. Jambor	75-1 to -8

Potassium and sodium began to migrate significantly after 50 seconds of beam exposure. To eliminate errors due to alkali mobility, the concentrations of K and Na were always determined first; counting periods for all elements were limited to 40 seconds, and the beam position was moved by 2–3 μm every 80 seconds to prevent sample decomposition. With these analytical conditions, the following limits of detection apply: Na 0.05, Al 0.02, Y 0.04, Dy 0.15, and Ce, Nd, Er, Yb 0.1 wt.%.

Beryllium and water cannot be determined by electron-microprobe analysis. Consequently, the compositions of yttrian milarite are treated here on an anhydrous basis, and Be was calculated to fill the (Al + Be)-populated *T*(2) sites (*cf.* "Chemical Composition" below). Structure refinement of

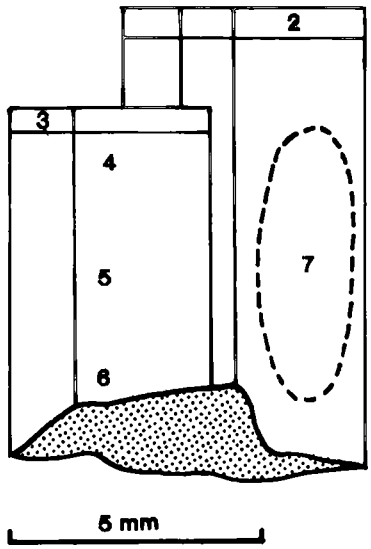

FIG. 1. Schematic view of a subparallel aggregate of milarite crystals from Jaguaraçú, Brazil, with locations of fragments examined in the present study. Numbers correspond to those in Tables 1, 2 and 3.

some of the analyzed samples shows that the Be contents derived from electron densities at the *T*(2) sites are in good agreement with those calculated here (Hawthorne *et al.* 1991).

Unit-cell dimensions of the Jaguaraçú milarite were calculated from X-ray powder-diffraction data obtained with a Philips PW1710 X-ray diffractometer, using graphite-monochromated Cu$K\alpha$ radiation at 40 kV and 40 mA, with a scan speed of 0.5° 2θ/min and annealed CaF_2 (*a* 5.46379(4) A; Ercit 1986) as an internal standard. From 13 to 22 powder reflections between 10° and 60° 2θ were used for the least-squares refinement, using a modified version of the program CELREF (Appleman & Evans 1973). Because of a very limited quantity of material, the Strange Lake milarite SL-60D-18.3 was X-rayed with a 114.6-mm Debye-Scherrer camera using Fe-filtered Co$K\alpha$ radiation; intensities were estimated from a 114.6-mm Gandolfi camera film obtained after additional material was added to the original spindle mount. A modified least-squares program (Gabe *et al.* 1989) was used to refine unit-cell dimensions from 19 diffraction maxima between 3.206 and 1.697 A. Unit-cell dimensions of the Strange Lake milarite SL-258-71, and other structural data from single-crystal fragments, were obtained on a Nicolet R3m automated four-circle diffractometer, using graphite-monochromated Mo$K\alpha$ radiation at ~50 kV and 35 mA.

Chemical composition

Yttrian milarite is chemically very heterogeneous in samples from both localities examined in the present study. Concentric zoning, sector zoning and replacement veining all are observed, both individually and in combination.

The Jaguaraçú milarite exhibits thin subsurface zones of increased (Y,*REE*) contents on the prismatic faces (Figs. 2A,D), rarely with a reversal to reduced (Y,*REE*) contents (Fig. 2B). This zoning is broader but not so (Y,*REE*)-enriched in the clear (001) caps of these crystals (Fig. 2C). The main body of each crystal is veined by (Y,*REE*)-rich milarite that corresponds in chemical composition to the (Y,*REE*)-rich subsurface zones (Figs. 2A,B,D). This network of veinlets extends from the subsurface zones, follows fractures in the homogeneous primary milarite, and is clearly a replacement, not a fissure-filling.

Milarite crystals from Strange Lake sample SL-258-71 show concentric zonal growth, with two distinct (Y,*REE*)-rich compositions that predominate over a (Y,*REE*)-poor composition. This latter composition is also dispersed in somewhat irregular streaks parallel to *c* throughout most of the crystal (Fig. 2E). The crystals also are corroded parallel to *c*, with the (Y,*REE*)-rich cores having been preferentially attacked; the outer zones, however, remain relatively unaffected.

Milarite crystals from Strange Lake sample SL-258-75.2 display sector zoning, with oscillatory compositional variations within the sectors (Fig. 2F). The (100) growth sectors are distinctly more enriched in (Y,*REE*) than are the sectors underlying the (001) pinacoids.

Table 2 lists the results of electron-microprobe analyses representative of the milarite occurrences examined; some of the analyzed spots are marked in Figure 2. A complete set of compositional data collected during this study is available from the Depository of Unpublished Data, CISTI, National Research Council of Canada, Ottawa, Ontario K1A 0S2.

All crystals show similar compositional trends, irrespective of locality. The broadest and most informative range of data is provided by the Jaguaraçú milarite, whereas the data for the Strange Lake milarite are much more restricted. Figure 3A shows a well-defined negative correlation between Ca and (Y + *REE*), and Figure 3B shows a poorer but statistically significant positive correlation of (Y + *REE*) with Be/(Be + Al). The Be/(Be + Al) ratio also is affected by the substitution

$$^{B}Na^{+} + {}^{T(2)}Be^{2+} \rightarrow {}^{B}\square + {}^{T(2)}Al^{3+}$$

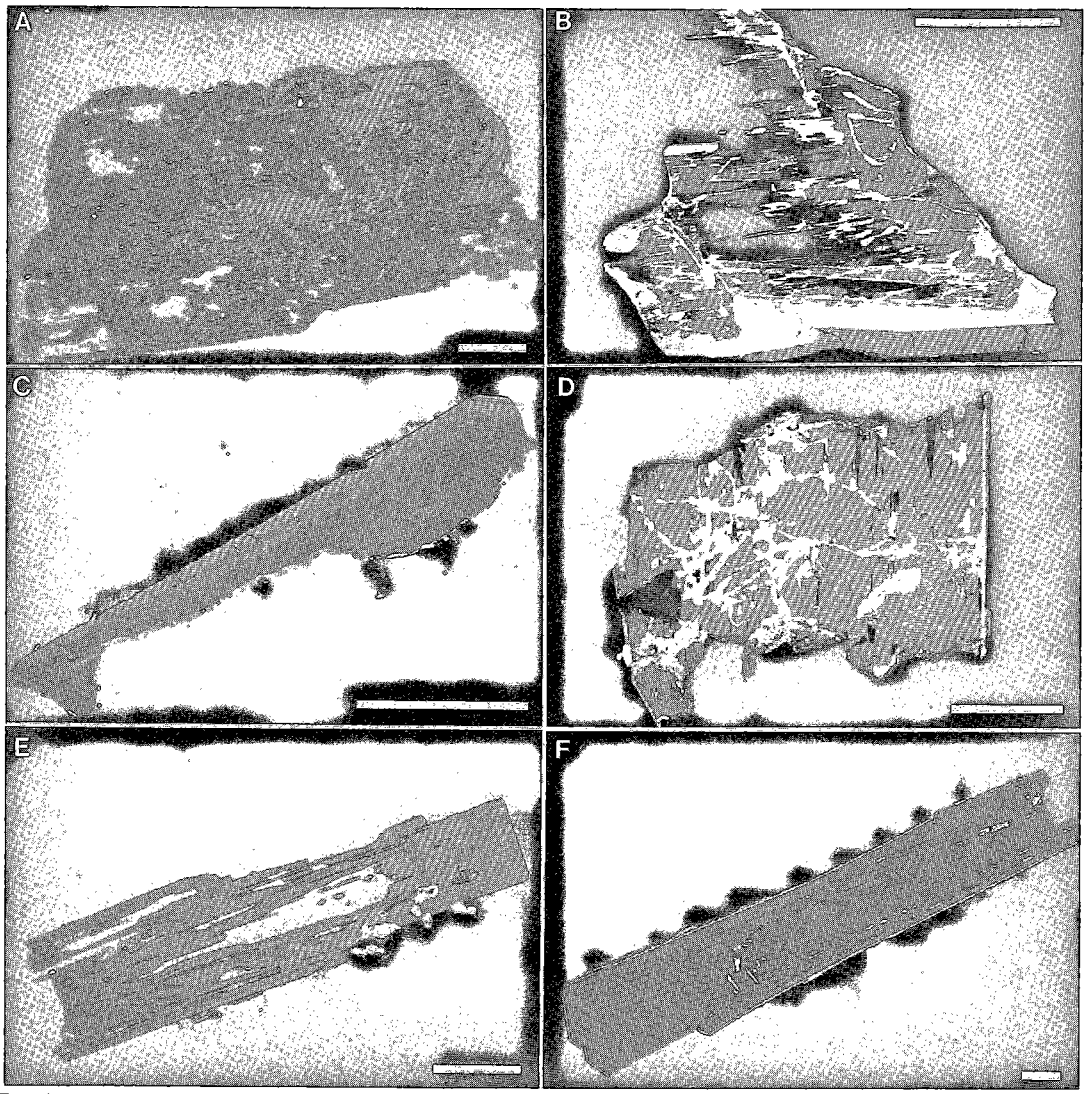

FIG. 2. Back-scattered electron images of yttrian milarite; light tones indicate increased contents of (Y,*REE*). A: Jaguaraçú, (Y,*REE*)-enriched subsurface zone and veining, *c* direction subhorizontal. B: Jaguaraçú, oblique section with reversal of primary zoning along the lower edge. C: Jaguaraçú, zoning in the clear cap. D: Jaguaraçú, (Y,*REE*)-enriched subsurface zone and veins, *c* direction vertical. E: Strange Lake SL–258–71, concentric zoning, (Y,*REE*)-poor streaks, and corrosion; bright spots mark inclusions of probable titanite. F: Strange Lake SL–258–75.2, sector zoning. Scale bars equal 1 mm (A to D) and 0.1 mm (E and F).

(Černý *et al.* 1980); thus we do not expect the data to fall along the ideal line in Figure 3B, as the analytical data also indicate significant variations in the extent of this (Y, *REE*)-free substitution.

The cation contents corresponding to the chemical compositions given in Table 2 were calculated on the basis of 30 oxygen anions (excluding H_2O) with the constraint that Be + Al equal 3.00 apfu (atoms per formula unit). It is obvious that some kind of systematic error is present, either in the analytical data or in our understanding of the milarite structure. First, the Si content exceeds the ideal value of 12.00 apfu, and this observed excess shows a positive correlation with the (Y,*REE*) content. Adjustment of the SiO_2 wt.% of several compositions to produce 12.00 apfu Si brings the

TABLE 2. CHEMICAL COMPOSITION

Locality	Jaguaraçú					Strange Lake				
Analysis	MI-B-1	MI-B-2	MI-2-2	MI-7-1	MI-7-2	71-1	71-2	75-1	75-6	75-8
SiO_2	70.00	73.40	72.70	73.20	70.00	71.20	70.20	71.00	70.00	70.00
Al_2O_3	0.23	5.10	3.40	4.70	0.13	0.40	0.04	1.90	n.d.	0.15
BeO	7.11	5.10	5.86	5.29	7.15	7.15	7.24	6.41	7.22	7.13
CaO	6.40	10.90	9.50	11.10	6.40	7.00	5.60	8.70	6.30	6.40
Na_2O	0.19	n.d.	n.d.	n.d.	0.12	0.16	n.d.	0.07	0.19	n.d.
K_2O	4.70	4.80	5.10	4.90	4.70	4.50	4.50	5.20	4.80	5.10
Y_2O_3	5.20	n.d.	1.80	n.d.	5.80	6.20	7.90	2.90	5.60	3.60
Ce_2O_3	n.d.	n.d.	n.d.	n.d.	n.d.	n.d.	0.40	0.40	0.10	2.20
Nd_2O_3	0.20	n.d.	n.d.	n.d.	0.20	n.d.	0.30	0.20	0.10	0.70
Dy_2O_3	0.50	n.d.	0.20	n.d.	0.70	0.60	0.90	0.30	0.50	0.50
Er_2O_3	0.80	n.d.	0.20	n.d.	0.70	0.50	0.80	0.20	1.10	0.60
Yb_2O_3	2.40	n.d.	0.60	n.d.	1.30	0.30	0.50	0.20	1.90	1.10
total	97.73	99.30	99.36	99.19	97.20	98.01	98.38	97.48	97.81	97.48
Si	12.104	12.045	12.062	12.037	12.112	12.107	12.071	12.072	12.100	12.140
Al	0.047	0.986	0.665	0.911	0.027	0.080	0.008	0.381	-	0.031
Be	2.953	2.011	2.336	2.090	2.972	2.921	2.991	2.618	2.998	2.970
Ca	1.186	1.917	1.689	1.956	1.187	1.275	1.032	1.585	1.167	1.189
Na	0.064	-	-	-	0.040	0.053	-	0.023	0.064	-
K	1.037	1.005	1.079	1.028	1.038	0.976	0.987	1.128	1.059	1.128
Y	0.478	-	0.159	-	0.534	0.561	0.723	0.262	0.515	0.332
Ce	-	-	-	-	-	-	0.025	0.025	0.006	0.140
Nd	0.012	-	-	-	0.012	-	0.018	0.012	0.006	0.043
Dy	0.028	-	0.011	-	0.039	0.033	0.050	0.016	0.028	0.028
Er	0.043	-	0.010	-	0.038	0.027	0.043	0.011	0.060	0.033
Yb	0.127	-	0.030	-	0.069	0.016	0.026	0.010	0.100	0.058
total	18.079	17.964	18.041	18.021	18.067	18.049	17.975	18.144	18.103	18.092
Be/(Be + Al)	0.984	0.671	0.778	0.696	0.991	0.973	0.997	0.873	1.000	0.990
Y + REE	0.688	0.000	0.210	0.000	0.692	0.637	0.885	0.336	0.715	0.634
Ca + Y + REE	1.874	1.917	1.899	1.956	1.879	1.912	1.917	1.921	1.882	1.823

MI-2-2: (Y,REE)-poor clear cap; MI-7-1 and -2: main body of the crystal (Fig. 3A); 71-1 and -2: darker and lighter area, respectively, of zoned crystal (Fig. 3E); 75-1, -6 and -8: darkest core, lightest zone in termination and most Ce-enriched spot, respectively, on the sector-zoned crystal (Fig. 3F). n.d. = not detected.

total oxide wt.% to well below ~98 wt.%, which is an average value for ideal milarite. This suggests that the problem is not due to errors in the SiO_2 determinations. Second, the Ca content of (Y,*REE*)-free samples still falls below the ideal value of 2.00 apfu by a factor of 1.04. This suggests that there is a systematic error in the Ca analyses, an error that we can remove by scaling the Ca content up by a factor of 1.04; we note that this also reduces the amount of excess Si in the calculated formula unit. However, with increasing (Y,*REE*) substitution, the *A*-site cation sum is still low, falling from a near-ideal value of 1.96 apfu at (Y,*REE*)-free compositions to ~1.82 apfu at (Y,*REE*)-rich compositions (Fig. 3C). Our limits of detection on the electron microprobe indicate that this discrepancy of ~0.18 apfu cannot be assigned to undetected light *REE*s. Thus, we are also forced to assume that a systematic error exists in our *REE* values, if we make the reasonable supposition that the *A* site has no vacancies. However, we have no reasons to doubt the quality of the microprobe standards or the reliability of any steps in the analytical procedure. Thus, the alternative possibility must be considered that Na or vacancies (or both) also are involved in the charge-balance mechanism in (Y,*REE*)-rich compositions. Whether systematic error or vacancies, neither affects the principal conclusion that Y and *REE*s are incorporated into the milatite structure primarily by the substitution $^{A}Ca^{2+} + {}^{T(2)}Al^{3+} \rightarrow {}^{A}(Y,REE)^{3+} + {}^{T(2)}Be^{2+}$.

An idealized substitution, ignoring the possible deviations from ideal occupancies of cation sites (which amount to a maximum of 9%, and generally less than 5%), indicates a trend from the ideal composition of milarite to an "end-member" counterpart with Ca/Y of 1.00, *i.e.*, from $KCa_2(Be_2Al)Si_{12}O_{30}$ to $K(CaY)(Be_3)Si_{12}O_{30}$.

X-ray diffraction

Table 3 lists X-ray powder-diffraction data for both the Strange Lake and Jaguaraçú samples of yttrian milarite, compared to those of the classic, optically "anomalous" milarite (Guanajuato #25) and the optically hexagonal milarite with positional disorder of Ca and increased *B*-site occupancy (Věžná #29; from Table 10 in Černý *et al.* 1980). Figure 4 shows the distinctly different distributions of intensities in the X-ray powder-diffraction patterns of all three types.

Whereas Černý *et al.* (1980) ascribed the differences in diffraction intensities between the

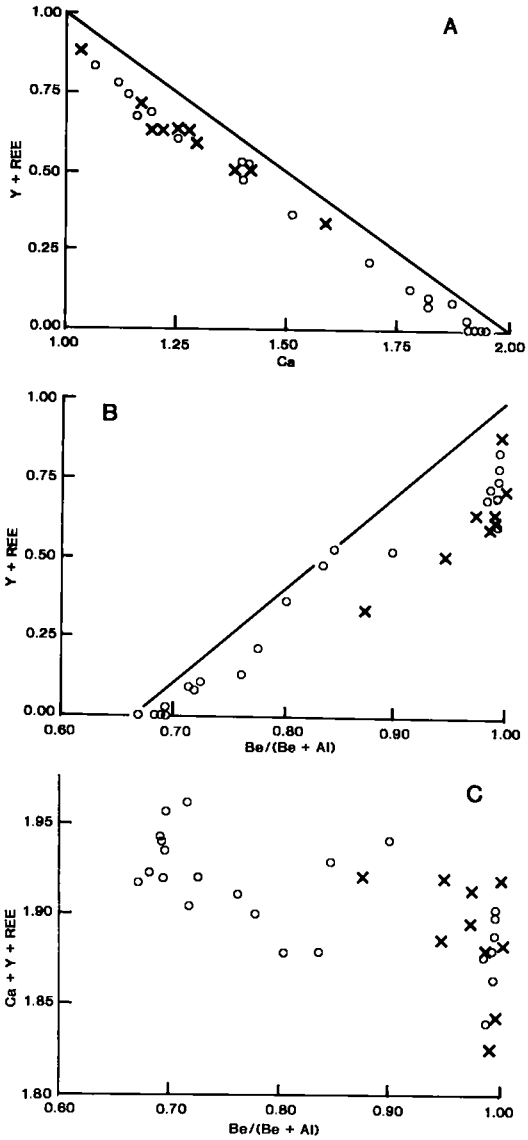

FIG. 3. A. Ca *versus* (Y + Σ*REE*) (apfu) in yttrian milarite. Note that the data plot consistently below the line that marks the ideal correlation. Circles: Jaguaraçú; X: Strange Lake. B. (Y + Σ*REE*) *versus* Be/(Be + Al) (apfu) in yttrian milarite. Note that the data plot below the line that marks the ideal substitution. Symbols as in Figure 3A. C. (Ca + Y + Σ*REE*) *versus* Be/(Be + Al) (apfu) in yttrian milarite. Difference between 2.00 and (Ca + Y + ΣREE) equals "vacancies" in the *A* site. Symbols as in Figure 3A.

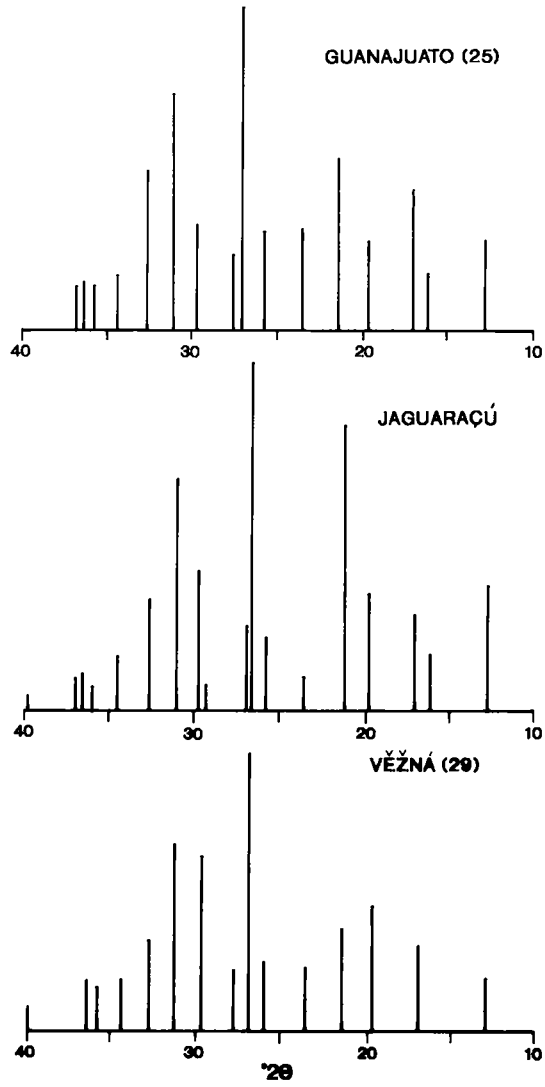

FIG. 4. X-ray powder diffractogram of Jaguaraçú milarite M1–7 compared to those of Guanajuato milarite #25 and Věžná milarite #29 (Černý *et al.* 1980).

Guanajuata and Věžná specimens to the higher alkali and H_2O content of the latter, the difference between these two and the Jaguaraçú yttrian milarite is not so easily clarified. The lack of quantitative data on H_2O contents of yttrian milarite is the main obstacle. Nevertheless, we expect that the substitution of Y (Z = 39) for Ca (Z = 20) at the A sites is in part responsible, as well as the increased Be/Al ratio at $T(2)$.

Unit-cell dimensions of yttrian milarite listed in Table 4 are compared with those of other samples of milarite in Figure 5. In Y-poor milarite, a and c decrease with increasing Be/Al at $T(2)$; c decreases and a increases with increasing H_2O (Černý *et al.*

TABLE 3. X-RAY POWDER-DIFFRACTION DATA

Milarite (25) Guanajuanto[1]				Milarite (29) Věžná[1]				Milarite SL-60D-18.3[2]				Milarite MI-7[3]			
I_{meas}	$d(Å)_{meas}$	$d(Å)_{calc}$	hkl	I_{meas}	$d(Å)_{meas}$	$d(Å)_{calc}$	hkl	I_{meas}	$d(Å)_{meas}$	$d(Å)_{calc}$	hkl	I_{meas}	$d(Å)_{meas}$	$d(Å)_{calc}$	hkl
16	6.93	6.913	002	6	6.85	6.837	002	70	6.87	6.86	002	37	6.898	6.884	002
7	5.48	5.487	102	-	-	5.448	102	20	5.46	5.44	102	17	5.464	5.458	102
36	5.22	5.209	110	21	5.20	5.207	110	30	5.17	5.16	110	28	5.174	5.170	110
19	4.51	4.511	200	39	4.51	4.509	200	50	4.47	4.47	200	34	4.478	4.477	200
47	4.16	4.160	112	29	4.14	4.142	112	100	4.13	4.13	112	82	4.134	4.139	112
24	3.777	3.778	202	15	3.763	3.764	303	10	3.75	3.75	202	11	3.766	3.753	202
23	3.456	3.457	004	16	3.418	3.418	004	20	3.436	3.432	004	22	3.446	3.442	004
100	3.316	3.311	211	100	3.310	3.307	211	100	3.277	3.281	211	100	3.287	3.287	211
16	3.227	3.228	104	16	3.200	3.206	203	30	3.206	2.304	104	26	3.217	3.213	104
		3.224	203			3.196	104	100	3.031	3.031	212	8	3.037	3.037	212
27	3.009	3.007	300	60	3.007	3.006	300	50	2.977	2.980	300	40	2.985	2.983	300
71	2.882	2.880	114	65	2.858	2.858	114	100	2.858	2.858	114	66	2.867	2.865	114
46	2.745	2.744	204	28	2.729	2.730	213	35	2.722	2.722	204	32	2.729	2.729	204
		2.741	213			2.724	204			2.718	213		-	-	-
9	2.603	2.604	220	13	2.603	2.603	220	25	2.580	2.581	220	16	2.583	2.585	220
8	2.511	2.519	303	10	2.504	2.509	303	10	2.481	2.479	310		-	-	-
		2.502	310			2.501	310					7	2.485	2.483	310
10	2.462	2.462	311	13	2.460	2.460	311	10	2.440	2.440	311	11	2.443	2.444	311
9	2.431	2.437	222	4	2.420	2.433	222	15	2.416	2.415	222			-	-
		2.427	214			2.414	214					10	2.417	2.413	214
1	2.265	2.269	304	3	2.255	2.257	304	5	2.248	2.250	304		-	-	-
-	-	-	-	-	-	-	-	3	2.228	2.235	400	-	-	-	-
6	2.198	2.199	313	7	2.193	2.193	313	10	2.179	2.180	313	7	2.185	2.184	313
1	2.149	2.148	215	1	2.132	2.133	215	3	2.136	2.131	215		-	-	-
3	2.107	2.107	116	3	2.090	2.088	116	20	2.092	2.092	116	7	2.095	2.097	116
-	-	-	-	-	-	-	-	5	2.060	2.063	224	-	-	-	-
3	2.045	2.047	321	5	2.044	2.046	321	10	2.033	2.028	321	-	-	-	-
11	2.026	2.027	314	9	2.019	2.018	314	20	2.007	2.010	314	10	2.013	2.012	403
7	1.967	1.969	410	13	1.967	1.968	410	25	1.953	1.951	410	14	1.951	1.954	410
3	1.950	1.949	411	3	1.945	1.948	411	3	1.934	1.931	411		-	-	-
12	1.890	1.894	412	8	1.886	1.891	412	30	1.875	1.876	412	17	1.878	1.879	412
		1.889	404			1.884	323	-	-	-	-	-	-	-	-
		1.888	323			1.882	404	-	-	-	-	-	-	-	-
14	1.855	1.855	315	12	1.846	1.846	315	20	1.840	1.840	315	13	1.844	1.845	315

[1] From Černý et al. (1980); [2] 114.6 mm Debye-Scherrer camera; [3] PW-1710 diffractometer; average for compositions MI-7-1 and MI-7-2 given in Table 2.

1980). In unheated natural Y-poor milarite, the increase in Be/Al and H_2O is roughly parallel. The combined effects of these two variables result in nearly constant values of *a* (opposite effects of Be/Al and H_2O), but in a considerable range in *c* (compounded effects of both).

The *a* dimension of yttrian milarite is distinctly smaller than that of the other types of milarite, and the *c* dimension falls in the middle of the known range (Fig. 5). It is again difficult to interpret these differences in detail because the contents of H_2O are not known. However, the samples of yttrian milarite examined in the present study all have a very high Be/Al ratio, which should reduce the size of the *T*(2) tetrahedra. Also, the smaller ionic radius of Y^{3+} relative to that of Ca^{2+} (0.90 *versus* 1.00 Å for octahedral coordination: Shannon 1976) should reduce the size of the *A* octahedra. The *A* and *T*(2) polyhedra must lead to a reduction in both *a* and *c* cell dimensions, but particularly the former: unit-cell dimensions of (Y,*REE*)-enriched milarite decrease in this manner relative to the ideal composition, in which Be/(Be + Al) equals 0.66 (*cf.* Fig. 5). This qualitative argument is in agreement with the results of structure refinements on the Jaguaraçú and Strange Lake material (Hawthorne *et al.* 1991).

TABLE 4. UNIT-CELL DIMENSIONS

	a(Å)	c(Å)	V(Å^3)	Method
(Y,REE)-enriched milarite				
MI-7	10.339(3)	13.768(5)	1274.7(7)	Philips PW 1710
MI-7	10.342(2)	13.777(6)	1275.8(9)	Nicolet R3m
SL-60D-18.3	10.325(5)	13.725(8)	1267.0(1.9)	114.6mm camera
SL-258-71	10.340(1)	13.758(2)	1273.9(4)	Nicolet R3m
Milarite close to $KCa_2(Be_2Al)Si_{12}O_{30}$ (Černý et al. 1980)				
#20	10.412(2)	13.823(5)	1294.5(5)	Philips 1352
#22	10.404(3)	13.819(7)	1295.4(7)	Philips 1352
#25	10.408(2)	13.826(6)	1297.1(6)	Philips 1352

For details of data collection, see "Experimental Methods".

CONCLUSIONS

The present study shows that substantial amounts of Y and (*H*)*REE* can enter the octahedrally coordinated *A* site of the milarite structure, normally occupied by Ca. This substitution is charge-balanced by increased Be/Al at the *T*(2) site, or possibly by a slight reduction in (K,Na) at the C and B sites relative to their contents

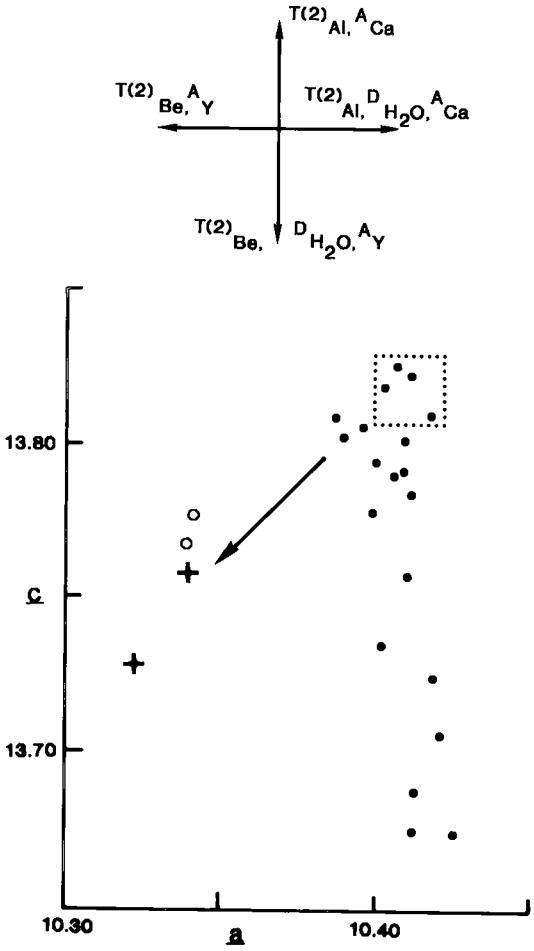

FIG. 5. Unit-cell dimensions of milarite samples close to the $Be^{2+} + Na^{+}$ $Al^{3+} + \square$ substitution series (Černý *et al.* 1980) compared to those of yttrian milarite. Dotted rectangle marks unit-cell dimensions characteristic of the composition $KCa_2(Be_2Al)Si_{12}O_{30}$. Vectors parallel to the coordinates indicate changes in unit-cell dimensions resulting from different substitutions. Arrow indicates reduction in unit-cell dimensions from the $KCa_2(Be_2Al)Si_{12}O_{30}$ composition to the Jaguaraçú (circles) and Strange Lake (crosses) milarite.

expected in (Y,*REE*)-free milarite. The substitution $^{A}(Y,REE)^{3+} + {}^{T(2)}Be^{2+} \leftrightharpoons {}^{A}Ca^{2+} + {}^{T(2)}Al^{3+}$ strongly modifies the intensities of the X-ray powder-diffraction maxima, and also affects both unit-cell dimensions. Despite an apparent slight deficit in the (Ca,Y,*REE*) population of the *A* site, this substitution generates a compositional series from the ideal milarite composition $KCa_2(Be_2Al)Si_{12}O_{30}$ to an Al-free "end-member" $K(CaY)Be_3Si_{12}O_{30}$.

Milarite from (Y,*REE*)-poor parageneses typically contains minor quantities of Y. This fact, plus its high Y,(*H*)*REE* contents in lanthanide-rich environments, indicate that milarite is a sink for these elements. Additional occurrences of yttrian milarite can be expected, particularly in vugs and fissures of peralkaline intrusive bodies similar to the Grorud nordmarkite in Norway, and in hydrothermal orebodies related to alkaline intrusive complexes of the Strange Lake type, such as the Blachford Lake complex in the Northwest Territories (Trueman *et al.* 1988). The Jaguaraçú granitic pegmatite seems to be too much of a geochemical oddity (enriched in both rare alkalis and Y,*REE*) to predict further finds of yttrian milarite in granitic pegmatites in general.

It is quite possible that the composition of yttrian milarite will extend into the $K(CaY)Be_3Si_{12}O_{30}$ – $(Y_2)(Be_3)Si_{12}O_{30}$ range at one or another locality, defining a new species with Y > Ca.

ACKNOWLEDGEMENTS

The authors thank Dr. R.V. Gaines for the Jaguaraçú specimens. Extensive help was provided by Mr. D. Teertstra in dissection and separation of the samples examined, and by Mr. N. Ball during the X-ray-diffraction work. This research was supported by NSERC Operating and Equipment grants to P.Č. and F.C.H. Technical assistance was kindly provided by D.R. Owens, J.H.G. Laflamme, P. Carrière and E.J. Murray at CANMET, and by A.C. Roberts at Geological Survey of Canada. Critical reviews by T. Armbruster, A.C. Roberts and R.F. Martin considerably improved the presentation.

REFERENCES

APPLEMAN, D.E. & EVANS, H.T., Jr. (1973): Job 9214: indexing and least-squares refinement of powder diffraction data. *U.S. Geol. Surv., Comp. Contrib.* **20** *(NTIS Document* PB2–16188).

ARMBRUSTER, T., BERMANEC, V., WENGER, M. & OBERHÄNSLI, R. (1989): Crystal chemistry of double-ring silicates: structure of natural and dehydrated milarite at 100 K. *Eur. J. Mineral.* **1**, 353-362.

BOILY, M., WILLIAMS-JONES, A.E. & SALVI, S. (1990): A reappraisal of the geology and geochemistry of the Zr–Y–Nb–Be and *REE* mineralized Strange Lake peralkaline pluton, Quebec–Labrador. *Geol. Assoc. Can. - Mineral. Assoc. Can., Program Abstr.* **15**, A13.

ČERNÝ, P. (1960): Milarite and wellsite from Věžná.

Práce Brněn. Základny ČSVA **32**, 1, No. 399, 1-14 (in Czech).

_____ (1967): Notes on the mineralogy of some West-Moravian pegmatites. *Cas. pro Mineral. a Geol.* **12**, 461-463 (in Czech).

_____ (1968): Berylliumminerale in Pegmatiten von Věžná und ihre Umwandlungen. *Ber. deutsch. Ges. Geol. Wiss. B* **13**, 565-578.

_____, HAWTHORNE, F.C. & JAROSEWICH, E. (1980): Crystal chemistry of milarite. *Can. Mineral.* **18**, 41-57.

CHISTYAKOVA, M.B., OSOLODKINA, G.A. & RAZMANOVA, Z.P. (1964): Milarite from central Kazakhstan. *Dokl. Akad. Nauk S.S.S.R.* **159**, 1305-1308 (in Russ.).

ERCIT, T.S. (1986): *The Simpsonite Paragenesis: the Crystal Chemistry and Geochemistry of Extreme Ta Fractionation.* Ph.D. thesis, Univ. Manitoba, Winnipeg, Manitoba.

FOORD, E.E., GAINES, R.V., CROCK, J.G., SIMMONS, W.B., JR. & BARBOSA, C.P. (1986): Minasgeraisite, a new member of the gadolinite group from Minas Gerais, Brazil. *Am. Mineral.* **71**, 603-607.

GABE, E.J., LE PAGE, Y., CHARLAND, J.-P., LEE, F.L. & WHITE, P.S. (1989): NRCVAX - an interactive program system for structure analysis. *J. Appl. Crystallogr.* **A22**, 384-387.

HAWTHORNE, F.C., KIMATA, M., ČERNÝ, P., BALL, N. & GRICE, J.D. (1991): The crystal chemistry of the milarite group minerals. *Am. Mineral.* (in press).

IOVCHEVA, E.I., KUPRIYANOVA, I.I. & SIDORENKO, G.A. (1966): Milarite from central Asia. *Dokl. Acad. Sci. U.S.S.R., Earth Sci. Sect.* **170**, 160-163.

JANECZEK, J. (1986): Chemistry, optics, and crystal growth of milarite from Strzegom, Poland. *Mineral. Mag.* **50**, 271-277.

KIMATA, M. & HAWTHORNE, F.C. (1989): The crystal structure of milarite: two split-site models. *Ann. Rept. Univ. Tsukuba* **15**, 92-95.

MILLER, R.R. (1989): Peralkaline granite-hosted rare metal mineralization in the Strange Lake deposit, Labrador, Canada. *Int. Geol. Correlation Program, Project IGCP 217 Symp. Precambr. Granitoids (Helsinki), Abstr.* **90**.

NOVIKOVA, M.I. (1972): Milarite from Eastern Siberia. *Trudy Mineral. Mus. Nauk S.S.S.R.* **21**, 188-192 (in Russ.).

OFTEDAL, I. & SAEBØ, P. C. (1965): Contributions to the mineralogy of Norway. 30. Minerals from nordmarkite druses. *Nor. Geol. Tidsskr.* **45**, 171-175.

SHANNON, R.D. (1976): Revised effective ionic radii and systematic studies of interatomic distances in halides and chalcogenides. *Acta Crystallogr.* **A32**, 751-767.

SOSEDKO, T.A. (1960): An occurrence of milarite on the Kola Peninsula. *Dokl. Acad. Sci. U.S.S.R., Earth Sci. Sect.* **131**, 389-392.

_____ & TELESHEVA, R.L. (1962): Chemical composition of milarite. *Dokl. Acad. Sci. U.S.S.R., Earth Sci. Sect.* **146**, 112-114.

STANĚK, J. (1964): Milarite and triplite from the Marsíkov pegmatite in northern Moravia. *Acta Mus. Moraviae* **49**, 33-38 (in Czech).

TRUEMAN, D.L., PEDERSEN, J.C., DE ST. JORRE, L. & SMITH, D.G.W. (1988): The Thor Lake rare-metal deposits, Northwest Territories. *In* Recent Advances in the Geology of Granite-Related Mineral Deposits (R.P. Taylor & D.F. Strong, eds.). *Can. Inst. Min. Metall., Spec. Vol.* **39**, 280-290.

Received October 29, 1990, revised manuscript accepted March 18, 1991.